Power System Stability Analysis under Increasing Penetration of Photovoltaic Power Plants with Synchronous Power Controllers

Daniel Remon[1,*], Antoni M. Cantarellas[1,2], Juan Manuel Mauricio[3], Pedro Rodriguez[1,4]

[1]Department of Electrical Engineering, Technical University of Catalonia, 08222 Barcelona, Spain
[2]Abengoa, 41014 Seville, Spain
[3]Department of Electrical Engineering, University of Seville, 41092 Seville, Spain
[4]Department of Engineering, Loyola University Andalusia, 41014 Seville, Spain
[*]daniel.remon@estudiant.upc.edu

Abstract: The utilization of renewable sources brings many benefits to electric power systems, but also some challenges like the impact that renewable power plants employing power electronics have on the grid, which is gaining importance as the penetration of this type of generating stations increases, driven by the construction of large wind or solar photovoltaic power plants. This paper analyses the impact of large-scale photovoltaic power plants on a transmission grid for different penetration levels. The analysis considers power plants formed by a number of power converters employing synchronous power controllers, that allow them to have a harmonious interaction with the grid, and compares their performance with that of conventional power converter controllers, assuming in both cases that the power plants participate in frequency and voltage regulation. The study addresses both the small-signal stability of the system and its response to large disturbances that alter the active power balance and frequency stability. The results of the analysis show that photovoltaic power plants using synchronous power controllers are able to limit frequency deviations, improve the oscillation damping, and reduce the stress of other generating units, thus having a beneficial impact on the power system.

1. Introduction

Power generation systems employing renewable energy sources are gaining importance in power systems [1] and are expected to reach penetration levels over 30% in a near future, with the main contribution of wind and solar photovoltaic (PV) energy [2]. The presence of these generators has an impact on the steady state of a power system, altering traditional generation and power flow patterns, and on its dynamics, due to the variability of the primary resource and the characteristics of a grid connection based on power electronics.

With the expected increase of penetration of these systems, it is necessary to analyse the impact they have on the power system, and many studies, with different points of view, can be found in the literature. Thus, [3] reviews the impact that high penetration levels of wind energy have on different aspects of the design and operation of power systems; whereas [4] addresses power system planning, and determines optimal locations of wind power plants taking into account their impact on the performance of the power system. Other authors focus on the impact that variable sources have on the bulk power system generation and demand balance. For

instance, necessary changes in the energy dispatch to accommodate large amounts of PV are studied in [5], wind power curtailment is considered in [6], and several methods to reduce the active power fluctuations of PV plants are reviewed in [7]. The effects of distributed generators on distribution systems have also attracted the interest of many researchers, especially regarding voltage profiles and power flow reversal, but also addressing other topics like the interaction of distributed PV with distribution system equipment [8], or the harmonics introduced by this kind of systems [9].

Power system stability is also studied with multiple approaches. In this sense, works like [10] focus on low-voltage ride-through capability and short-term effects on voltage stability of PV systems, whereas other papers study the transient stability of a test power system with an important penetration of wind or PV [11,12]. The small-signal stability of a system with high rates of wind is also considered in [13], and is extended in some cases to the identification of subsynchronous resonance in the presence of series-compensated lines [14], whereas [15] addresses transient stability in a system with PV and identifies oscillatory phenomena.

Taking into account the reduction of total system inertia and regulation capability, system operators are usually concerned about the admissible penetration limits for these renewable systems. The impact of wind penetration on frequency regulation is studied in [16], and the combined effects of high penetrations of wind and PV in the frequency response of a power system are analysed in [17]. In order to overcome the issues originating from such high penetration scenarios, controllers that coordinate the response of conventional and alternative generators have been proposed [18], and the use of fast-responding storage systems is presented in [19] as a measure to compensate the loss of inertia in the system. Another approach is to control the power electronics systems interfacing renewable generators so they emulate the inertia of a synchronous machine, and [20] analyses the impact of wind turbines employing such a controller on a transmission system.

A further step in the development of these controllers is to reproduce not only the inertial effect of a synchronous machine but also its synchronous behaviour, resulting in what is called virtual synchronous machines, which have been implemented in many alternative ways, and using various names, by different authors. In this case, the analyses found in the literature present a particular design of the controller and the main traits of its dynamic behaviour, and the tests are normally restricted to a simple system where the power converters are connected to the main grid or to a small microgrid [21–28]. Namely, a virtual synchronous generator is connected to the low voltage distribution grid in [21], and to a microgrid with wind and diesel generators in [22]; two virtual synchronous machines, together with two conventional synchronous machines, form a microgrid that can be connected to the distribution grid in [23]; a synchronverter is connected to the

low voltage distribution network in [24]; the controller proposed in [25] is tested in an isolated grid with one synchronous machine through simulation, and connected to the distribution grid in an experimental setup; the performance of a hydro-PV microgrid is studied in [26]; and the synchronous power controller (SPC) is shown to operate connected and disconnected from the grid in [27], and its contribution to the stability of a microgrid is analysed in [28]. However, the impact of transmission-level power plants using this type of controllers is not considered.

Therefore, taking into account the fact that studies like those presented in [12,15,17] consider conventional power converter controllers for renewable power plants, or even constant power models in the case of PV, there is a gap of knowledge about the effects that renewable power plants of the order of hundreds of megawatts have on power system stability when they employ advanced controllers like virtual synchronous machines. In particular, the impact on the power system frequency response and the damping of power oscillations should be analysed. In order to cover this gap, in this paper, the stability of a transmission system is analysed under the presence of PV power plants using virtual synchronous machines. These plants are formed by a number of power converters whose control is based on the synchronous power controller [27, 29], for which equivalent aggregated models for power system analysis are already available [30], although similar conclusions could be reached for other virtual synchronous machine implementations. The study is performed on a test power system, proposed in [31,32], and comprises both its small-signal stability and its response to large disturbances affecting its frequency stability in a short range of time for which solar radiation can be considered constant. The analysis assesses how the penetration of PV plants influences their impact on the power system, and thus considers different PV penetration scenarios defined by the connection of an increasing number of 100 MW PV plants, which are represented by the equivalent model in [30].

2. Power Plant Model

The PV power plants considered in this paper are formed by 100 power conversion units of 1.1 MVA each and are modelled for balanced RMS analysis by means of an equivalent aggregated model [30]. This equivalent model allows both small- and large-disturbance analysis and takes into account the internal plant network and the dynamics of the power converters forming the PV plant. Through this equivalent model, each plant is represented by a single converter connected behind an equivalent impedance, obtaining the same results at the point of interconnection (POI). Considering the power and current ratings of the original power plant converters, the equivalent aggregated converter at the plant level has a steady-state apparent power limit of

110 MVA, and a transient current limit corresponding to 125 MVA at the rated voltage. Furthermore, this equivalent converter inherits the control of the original power plant converters, which is based on the SPC. In addition to the converter controller, a central plant controller handles the references and measurements at the POI of the power plant.

2.1. The Synchronous Power Controller

The SPC [27] makes power converters interact with the grid harmoniously like synchronous machines. In order to do that, it reproduces the simple model of a voltage source connected behind a virtual admittance, where the voltage source plays the role of the electromotive force (EMF) of a virtual synchronous generator. This is achieved by three main control blocks.

The first of these blocks generates the phase-angle of the EMF. This block defines the electromechanical behaviour of the controller and naturally synchronizes it with the grid by reproducing a swing equation with damping, such as:

$$2H\omega\frac{d\omega}{dt} = P_{in} - P_{out} - D\Delta\omega, \tag{1}$$

where ω is the rotor speed, H is its inertia constant in seconds, D is its damping, and P_{in}, P_{out} determine the power balance, with all magnitudes in per unit (p.u.). The frequency and phase-angle of the voltage source are thus obtained from the virtual rotor speed. Furthermore, due to the natural synchronization achieved through the swing equation, these two variables can be employed by other blocks of the power converter control system, avoiding the need for an ancillary phase-locked loop (PLL).

The second block is a reactive power controller that modifies the magnitude of the EMF in order to control the reactive power. In this case, a proportional-integral controller is considered. Finally, the third block reproduces the electrical model of the controller and calculates the converter current reference as the current that would flow through the virtual admittance, taking into account the EMF magnitude and phase-angle calculated by the other two blocks, and the resulting voltage drop with respect to the terminal voltage measurement.

It is worth noting that the SPC parameters are flexible, and it is possible to consider different inertia, damping, or virtual admittance values according to the operating conditions, since they are not defined by physical elements as in a conventional synchronous generator. Furthermore, the inclusion of the virtual admittance provides additional degrees of freedom, since it decouples the internal electromotive force from the converter output voltage, and it is not constrained by the converter filter.

In addition to these blocks, frequency and voltage droop characteristics can be included in the controller,

respectively modifying the active and reactive power references. The frequency and voltage measurements can be local or received from the central plant controller. The complete control diagram, adapted for RMS modelling, can be seen in Fig. 1.

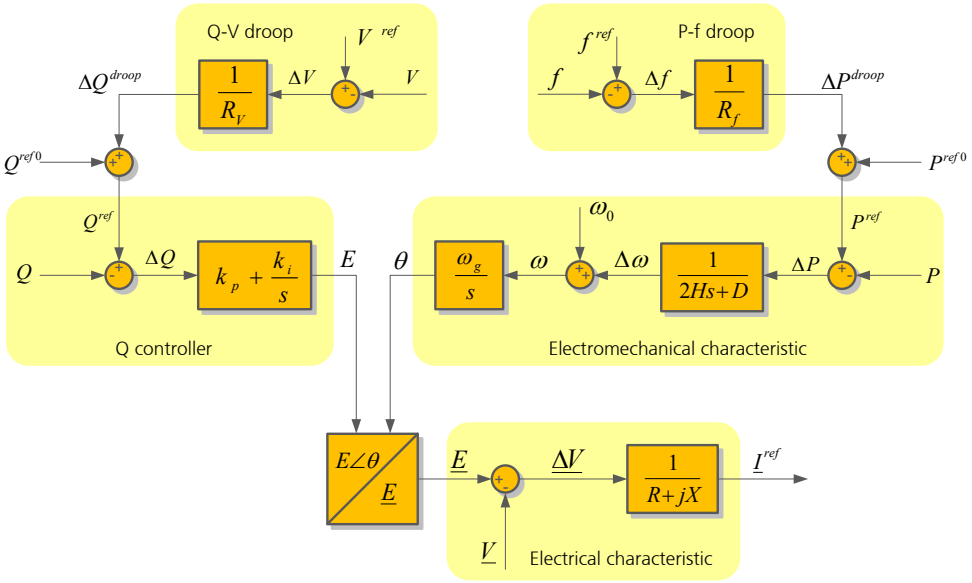

Fig. 1. *Model of the synchronous power controller employed by the PV power plant.*

Apart from the controller, the model of the power converter includes the current reference limiter, and the effect of the current loop is modelled as a first-order lag that takes into account its time constant, whereas faster dynamics of the inner controllers are considered instantaneous. Since the analysis focuses on short-term phenomena that do not involve radiation variations, the dynamics of the PV arrays and dc link are not considered in the model [33], but an active power reference limiter is included to avoid unrealistic active power injections for a PV system.

2.2. Power Plant Controller

The central plant controller generates the active and reactive power references to be followed by the equivalent converter and measures the frequency and voltage at the POI. The frequency measurement is obtained from a conventional PLL [34] connected at the POI, and filtered to remove high-frequency oscillations that are not of interest for primary frequency regulation.

In the tests carried out in this paper, the active power reference is kept constant and equal to 100 MW, whereas the frequency measurement is sent to the equivalent converter controller to be used only by the frequency droop controller. On the other hand, the voltage is controlled at the plant level by a proportional controller that generates a reactive power signal which is sent to the converter, keeping the converter voltage

droop disabled.

3. Test Power System and Scenarios

The analysis of the impact of these PV plants is carried out on a 12-bus test power system [31]. The system is adapted following [32], where typical generator, exciter and governor models are selected to define a benchmark for renewable energy integration. In this benchmark, the generating units and their control systems are characterized by inertia constants in the range 3.2 s - 4.8 s, high-transient-gain excitation systems performing a proportional control of the voltage at the generator terminals, and a common frequency droop slope of 5%; whereas the dynamic model of loads is a constant impedance model. In addition, the control systems of generators 3 and 4 are completed with power system stabilizers using a simple model [35], defined by the parameters given in Table 1.

Table 1 Power System Stabilizer Parameters

Parameter	Symbol	Value
Stabilizer gain	K	2 p.u.
Washout time constant	T	10 s
Lead-lag numerator	T_1	0.8895 s
Lead-lag denominator	T_2	0.03 s
Output limiter	H_{lim}	0.2 p.u.

To analyse the impact of the PV plants depending on the total share of solar generation in the power system, four different solar scenarios are defined by gradually increasing the load and the number of PV plants connected to the system:

1. 0% PV scenario: Base case with four conventional generators and a total demand of 1450 MW.
2. 10% PV scenario: Both generation and demand increase by 200 MW with the connection of PV plants 1 and 2 at bus 5.
3. 30% PV scenario: The demand remains the same as in the 10% scenario but the share of PV increases another 400 MW after the connection of PV plant 3 at bus 5, PV plant 4 at bus 3 and PV plants 5 and 6 at bus 4.
4. 50% PV scenario: The demand increases by 200 MW and PV plants 7, 8 and 9 are installed at buses 3, 7 and 6, respectively.

The resulting single-line diagram of the 12-bus system, indicating the location of the PV plants, is shown in Fig. 2. These four scenarios are defined taking into account the evolution of power systems, with increasing renewable penetration, and can be considered respectively as a traditional power system totally based on conventional generators (case 1), a currently realistic case of PV penetration in some power systems (case 2), a prospective case in the near future with a 30% PV penetration level during certain hours of the day (case 3), and a futuristic scenario beyond the usual renewable penetration limits (case 4).

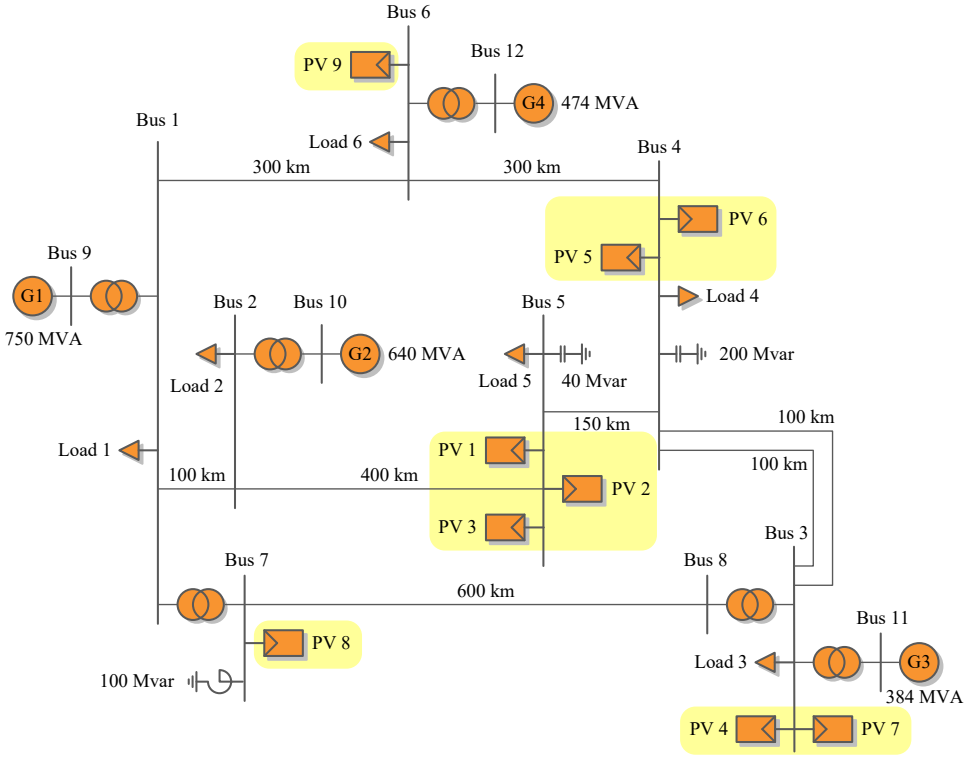

Fig. 2. *12-bus system diagram showing the points of interconnection of the PV power plants.*

In all the scenarios, generator 1 compensates the active power mismatch due to the losses in the system and the synchronous generators control the voltage at their terminals, i.e., at buses 9 to 12. The PV plants, on the other hand, control the voltage at their POI, sharing the reactive power reference evenly when several plants are connected at the same bus. The operating points of generators and loads that define the initial state of the system are summarized in Table 2, employing a base power of 100 MVA.

For each of the scenarios including PV, two different cases are considered in order to assess the real impact of power plants using synchronous power controllers. In the first case, the PV plants are controlled following a conventional strategy that includes controlling the voltage at the POI and contributing to frequency regulation through the frequency droop, but the converter controller is based on instantaneous power theory (IPT). In the RMS model, this means that the current reference is obtained from the division of the reference apparent

Table 2 Operation Scenario Definition for Different PV Penetration Levels

Element	Variable	0%	10%	30%	50%
G1	P (pu)	4.77	4.47	1.72	3.32
	V (pu)	1.00	1.00	1.00	1.00
G2	P (pu)	4.00	4.10	3.57	2.55
	V (pu)	1.01	1.01	1.01	1.01
G3	P (pu)	2.70	2.77	2.41	1.72
	V (pu)	1.01	1.01	1.01	1.01
G4	P (pu)	3.30	3.38	2.95	2.11
	V (pu)	1.01	1.01	1.01	1.01
Load 1	P (pu)	3.00	3.41	3.41	3.83
	Q (pu)	1.86	2.12	2.12	2.37
Load 2	P (pu)	2.50	2.84	2.84	3.19
	Q (pu)	1.21	1.38	1.38	1.54
Load 3	P (pu)	3.50	3.98	3.98	4.47
	Q (pu)	1.15	1.31	1.31	1.47
Load 4	P (pu)	3.00	3.41	3.41	3.83
	Q (pu)	1.86	2.12	2.12	2.37
Load 5	P (pu)	1.00	1.14	1.14	1.28
	Q (pu)	0.48	0.55	0.55	0.61
Load 6	P (pu)	1.50	1.71	1.71	1.91
	Q (pu)	0.49	0.56	0.56	0.63

power and the terminal voltage phasors. The second case considers the full PV plant model introduced in Section 2, with the SPC. For simplicity, the parameters that define the behaviour of the PV plants are given equal values for all the plants and scenarios. The main parameters are an inertia constant $H = 5$ s, counteracting the loss of inertia due to the connection of renewables with a slightly higher inertia constant than the synchronous machines in the system; an active power closed-loop damping ratio $\zeta = 0.7$, which provides additional damping for the power system response; a virtual reactance $X = 0.3$ p.u., allowing a close interaction between the SPC and the grid; and a frequency droop slope of 5%, so the PV plants contribute to frequency regulation in the same proportion as the synchronous generators.

4. Small-Signal Analysis

The amount and location of the PV plants connected to the power system and the type of controller employed by these plants have an impact on the modes that describe the system dynamics, and could affect the damping

of the oscillations that occur in the system.

The results of the analysis show that three modes can be identified as critical, with a damping ratio between 5% and 10% for most of the scenarios defined in Section 3; whereas the other modes have damping ratios over 20% and can be considered well damped. The eigenvalue plot in Fig. 3a and the data summarized in Table 3 allow studying the evolution of the critical modes under these scenarios. In general, increasing the number of PV plants in the system, and therefore the total frequency and voltage regulation capability, is beneficial for the system and results in a larger damping of the critical modes.

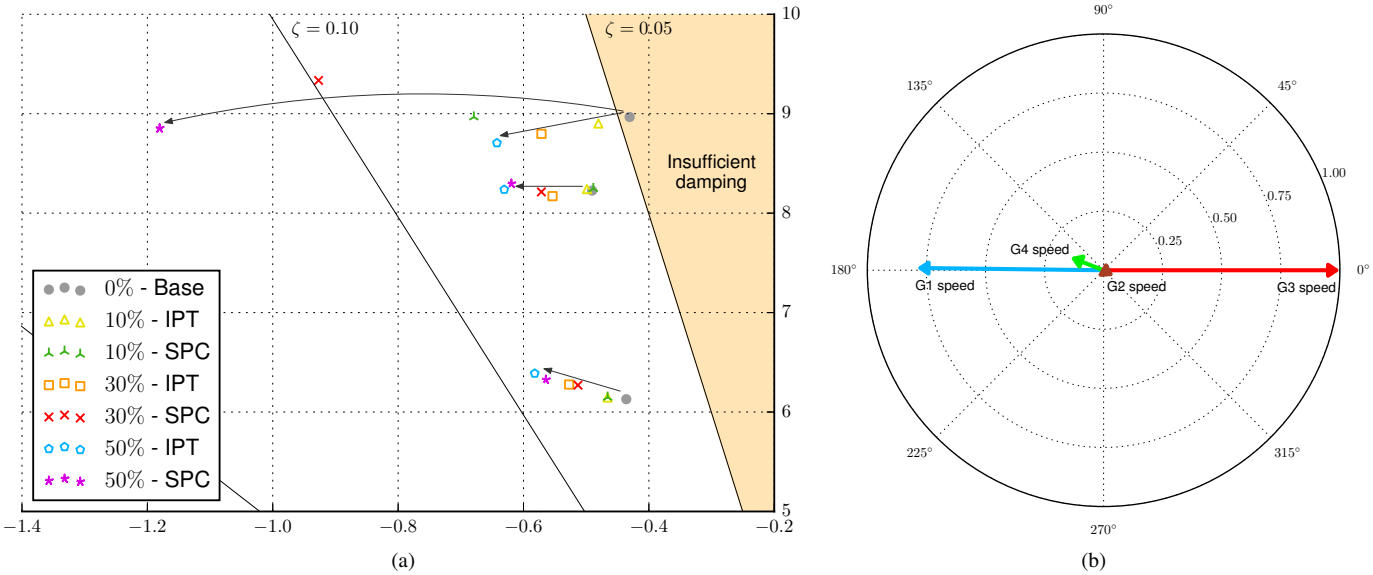

Fig. 3. *12-bus system eigenvalues. a) Critical eigenvalues for different scenarios. b) Controllability of mode 1 in the 0% PV scenario.*

Table 3 Critical 12-Bus System Eigenvalues and Damping Ratio for Different Scenarios

Scenario	Mode 1	Mode 2	Mode 3
0%	-0.4307 ± 8.9666 *j* 4.80%	-0.4905 ± 8.2269 *j* 5.95%	-0.4360 ± 6.1293 *j* 7.10%
10% - IPT	-0.4805 ± 8.9011 *j* 5.39%	-0.4988 ± 8.2419 *j* 6.04%	-0.4659 ± 6.1460 *j* 7.56%
10% - SPC	-0.6791 ± 8.9665 *j* 7.55%	-0.4884 ± 8.2466 *j* 5.91%	-0.4657 ± 6.1481 *j* 7.55%
30% - IPT	-0.5713 ± 8.7976 *j* 6.48%	-0.5536 ± 8.1709 *j* 6.76%	-0.5271 ± 6.2766 *j* 8.37%
30% - SPC	-0.9268 ± 9.3348 *j* 9.88%	-0.5714 ± 8.2136 *j* 6.94%	-0.5130 ± 6.2707 *j* 8.15%
50% - IPT	-0.6424 ± 8.7054 *j* 7.36%	-0.6307 ± 8.2373 *j* 7.63%	-0.5821 ± 6.3885 *j* 9.07%
50% - SPC	-1.1809 ± 8.8526 *j* 13.22%	-0.6197 ± 8.2964 *j* 7.45%	-0.5648 ± 6.3252 *j* 8.89%

Furthermore, the least damped mode, referred to as mode 1 in Table 3, shows a special sensibility to the type of PV controller. This mode corresponds to the inter-area oscillations between generators 1 and

3, as can be concluded from Fig. 3b, which shows the contribution of each synchronous generator to this mode. Taking into account the participating machines, it is reasonable that PV plants connected at buses 3, 4, and 5, which are near generator 3, have an important impact on this mode. In particular, its damping ratio improves significantly when the SPC is employed, reaching values of 9.88% and 13.22% for the 30% and 50% penetration scenarios, respectively; whereas it remains close to 7% when the IPT controller is used. On the other hand, the controller does not have an important effect on the other two critical modes.

Taking into account the least damped mode for each penetration level from Table 3, it can be concluded that the SPC makes possible to increase the minimum damping ratio of the modes in the system. This is mainly due to its effect on mode 1, that does not require an equivalent reduction of the damping of the other critical modes.

The impact on the system modes can also be seen in its time-domain response to a small disturbance. In this case, Fig. 4 shows the response of the system and PV plant 1 to a step variation in the voltage reference of generator 4, which is reduced from 1.01 p.u. to 1.00 p.u. at t = 1 s.

The system frequency is represented in Fig. 4a by the speed deviation of generator 2, which is one of the largest generators in the 12-bus system, and is connected at a central bus considering other generators and loads, as shown in Fig. 2. When the voltage reference of generator 4 is decreased, the consumption in neighbouring buses, which depends on the voltage, automatically decreases. This results in an excess of generation, which increases the system frequency. Due to the action of the primary frequency controllers, the average frequency is stabilized around a new value after 7 s. It is worth noting that the speed deviation is in all cases below $0.2 \cdot 10^{-3}$ p.u., which justifies the study in small-signal terms and allows focusing on the oscillatory behaviour due to the excitation of different power system modes.

This makes possible to observe some differences among scenarios. First, both the maximum deviation and the settling time of the response decrease as the PV penetration increases, which agrees with the results shown about the eigenvalues of the system in Table 3. Regarding the type of controller, the responses are very similar for both controllers in the 10% PV scenario, whereas the SPC achieves a slight damping improvement with respect to the IPT controller for a 30% penetration level, and a more appreciable beneficial effect in the 50% case.

In Fig. 4b, the voltage magnitude at bus 1, which is closer to the origin of the disturbance, is shown to have a similar behaviour under all scenarios, with oscillations during the first three seconds after the reference change, but within a close range around the initial value. The slight voltage variation in steady state, below

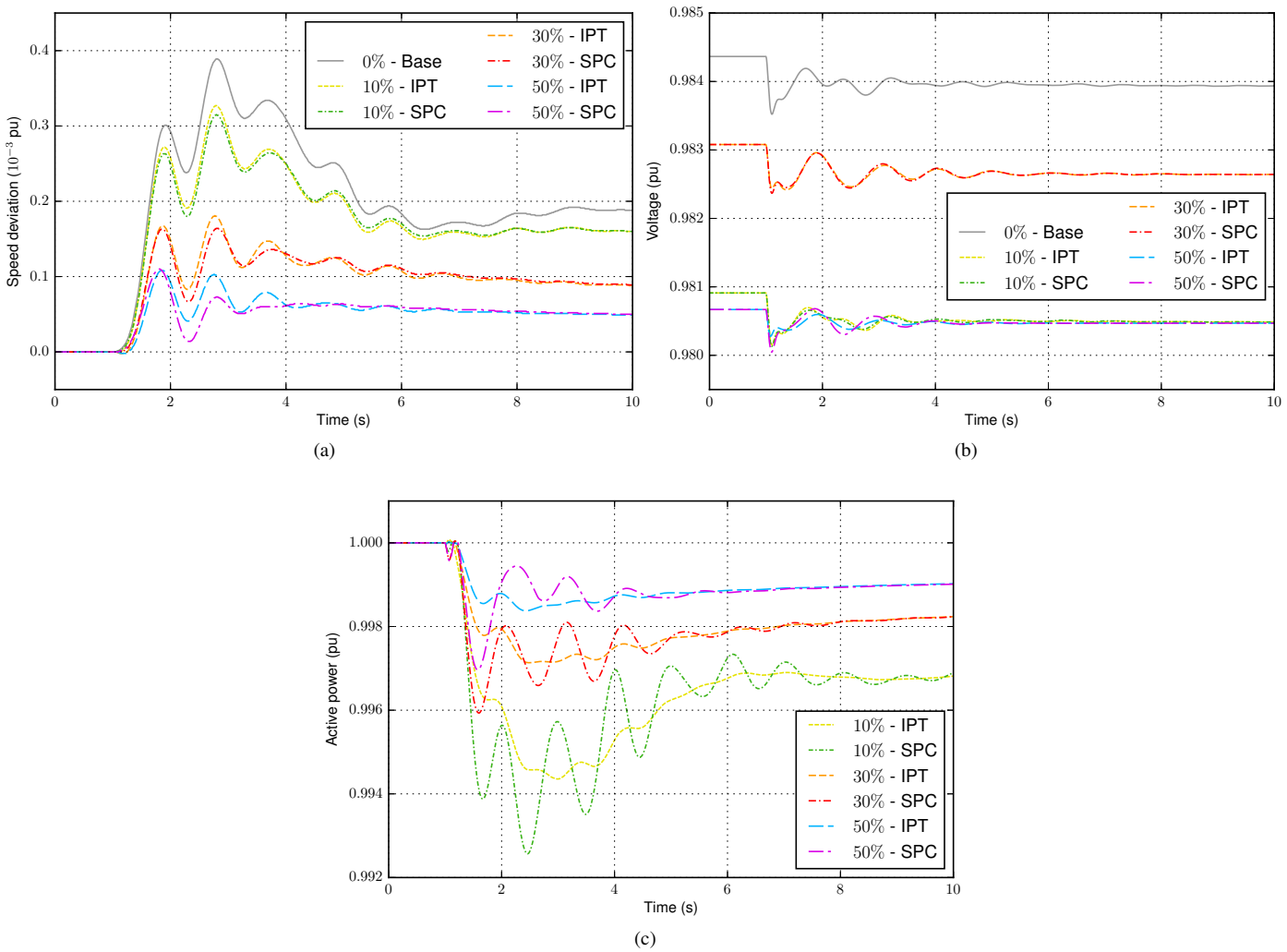

Fig. 4. *12-bus system response to a step in the voltage reference of generator 4. a) Generator 2 speed deviation. b) Bus 1 voltage. c) PV plant 1 active power.*

$0.5 \cdot 10^{-3}$ p.u. in all the scenarios, is due to the fact that the voltage is not directly controlled at bus 1, but at generator 1 terminals, and the voltage reference variation at generator 4 affects the neighbouring buses.

Fig. 4c shows the active power contribution of PV plant 1, connected at bus 5. Responding to the frequency increase, the active power injected by PV plant 1 decreases. The final active power variation is proportional to the frequency deviation and decreases when the penetration rises regardless of the type of controller. However, during the first seconds after the reference change, there are important differences depending on the PV plant controller. With the SPC, the PV plant absorbs part of the active power oscillations that the synchronous generators suffer during this event and contributes to damping them, more effectively as the number of PV plants increases.

5. Frequency Stability Analysis

This analysis will focus on the first few seconds after a large disturbance that alters the active power balance in the system, like the disconnection of a generator or a load, and will not address long-term effects. Therefore, the dynamics of interest are those of machines and their primary regulators, and a secondary controller that would modify the active power references of the generators in order to ensure that the frequency returns back to its nominal value is not considered.

5.1. Disconnection of a Generator

The first event studied in this analysis is the disconnection of generator 4 at t = 1 s. Depending on the scenario, this machine generates between 11% and 22% of the total active power in the 12-bus system and its disconnection causes a severe imbalance in the system before it reaches a new steady state, as can be seen in Fig. 5.

The speed of generator 2, which is used as a measurement of the system frequency, is shown in Fig. 5a. For a low penetration level of 10%, the presence of PV results in a deeper frequency fall than in the original case, and the speed of the response is approximately the same. However, in the 30% scenarios, although the maximum deviation is similar to the previous cases, the recovery is faster and the response is better damped. Finally, for a 50% penetration, the frequency deviation and the amplitude of the oscillations are reduced significantly as compared to the previous cases. As obtained from the eigenvalue analysis, the use of the SPC results in a better damping of the response for the 30% and 50% scenarios and, in the last case, also reduces the maximum frequency deviation.

All the generating units connected to the system react to this event to a greater or lesser extent. Fig. 5b shows the active power response of generator 2 for the 30% and 50% penetration cases. For these scenarios, the effect of the SPC on the damping of the oscillations is clearly beneficial and the stress of the synchronous machines is reduced. In this particular case, the amplitude of the oscillations in the active power generated by generator 2 after its first swing decreases by 0.05 p.u. to 0.10 p.u. when the SPC is employed, achieving relative amplitude reductions over 30% in the 50% penetration scenario.

On the other hand, Fig. 5c allows comparing the response of PV plant 1 in the different scenarios with PV. In all cases, the PV injection is around 1 p.u., but its behaviour depends on the type of controller used. With the controller based on IPT, the plant output power is almost constant before and after the event. However, when the SPC is employed, it naturally oscillates to counteract the frequency oscillations in the system. The

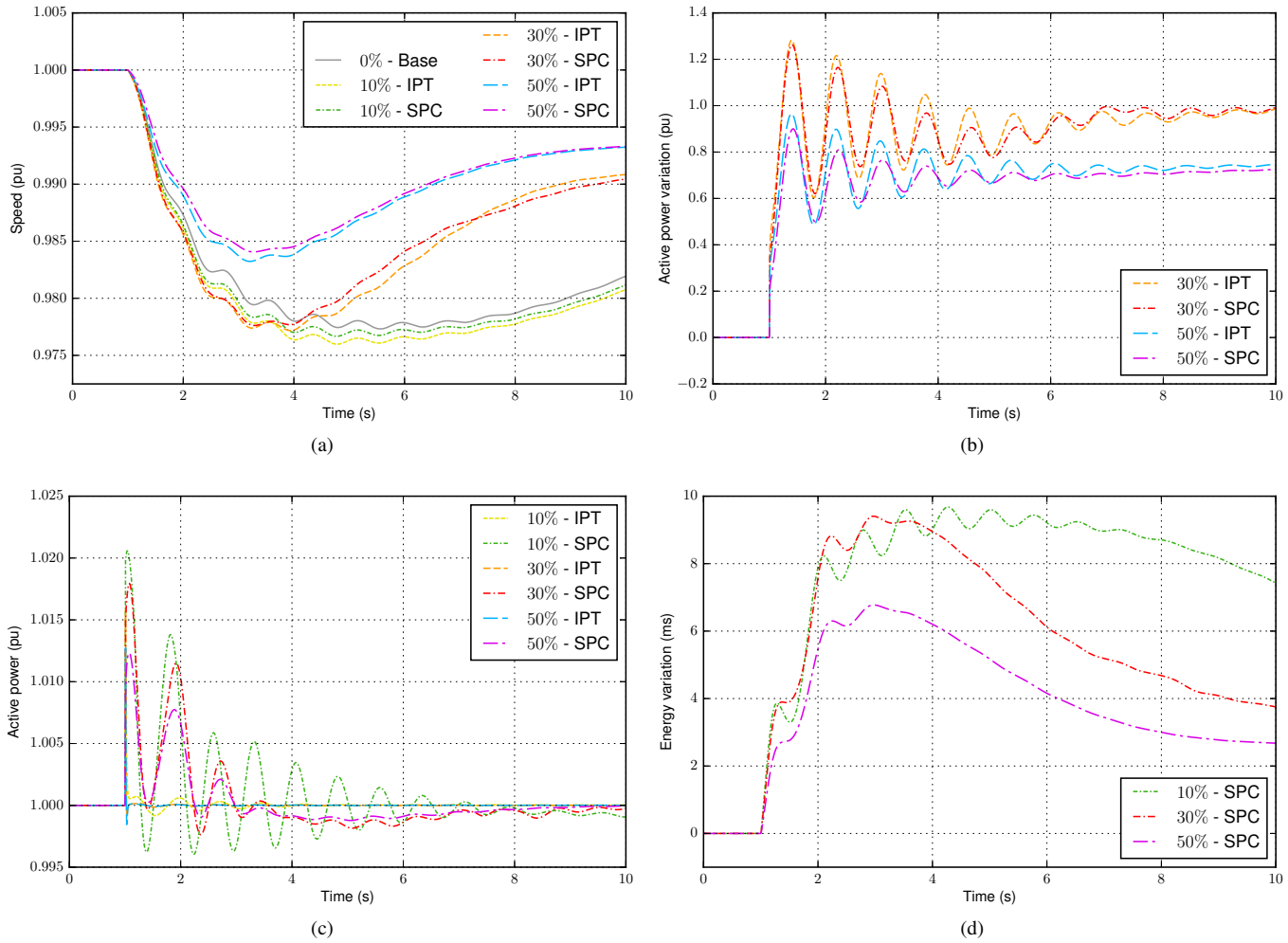

Fig. 5. *12-bus system response to the sudden disconnection of generator 4. a) Generator 2 speed. b) Generator 2 active power variation. c) PV plant 1 active power. d) PV plant 1 energy variation.*

amplitude and duration of the oscillations is larger when there are fewer PV plants connected to the system, like in the case of frequency.

These oscillations, which overload the PV plant, have a reduced amplitude and the maximum overload is around 2% for a few tenths of a second in the worst case. A power converter can safely withstand such an overload and the necessary active power can be extracted from the PV system as long as it is operating with a narrow reserve margin, or from a small, short-term storage device. The energy extracted from the PV equivalent converter after the disconnection of generator 4, expressed in time units considering the system base power, is shown in Fig. 5d for the scenarios where the SPC is employed. The energy variation depends on the system inertia and the parameters defining the SPC, and, for this severe event, the total amount of energy delivered by the plant is below 10 ms. As in the case of the oscillations, the amplitude of the energy variation decreases as the number of PV plants connected to the system increases. Taking into account the

little amount of energy involved, the necessary storage can be integrated in each converter through a proper design of its dc bus capacitance.

Therefore, there is a trade-off where oversizing the power plant PV field or the dc capacitance of the power converters results in an appreciable reduction of the torque oscillations suffered by the synchronous machines in the system, which contributes to reduce their mechanical and electrical wear.

5.2. Disconnection of a Load

The opposite event, i.e., the disconnection of a large load, is also considered in the analysis. In this case, load 4, connected at bus 4, is disconnected at t = 1 s. Opposing to generators, each load approximately represents the same share of the total demand under all the scenarios–around 21% for load 4–and the relative severity of the disconnection is similar for all the PV penetration levels. Therefore, in order to allow a better comparison of the responses depending on the type of PV controller employed, the following discussion focuses only on the results obtained for the highest PV penetration levels. Taking this into account, Fig. 6 shows the response of the system to this disturbance for the 30% and 50% PV penetration scenarios.

The frequency of the system, represented by the speed of generator 2 in Fig. 6a, exhibits relevant differences between both types of controllers. First, when the PV plants use the SPC, the frequency varies more slowly, due to the addition of their virtual inertia to the physical inertia of the synchronous generators. This reduces the response slope and delays the moment when it reaches its maximum deviation for approximately 1 s for both scenarios. Moreover, the response is more damped when the SPC is employed and, under the 50% scenario, the maximum speed deviation is visibly reduced, around 10%, without compromising the speed of the recovery.

Furthermore, the type of PV controller used by the PV plants also affects the response of the synchronous generators in the system, which suffer a more moderate reduction of their active power injection when the controller is virtually synchronous than when it is based on IPT, as shown in Fig. 6b for generator 2. In this figure, it is possible to observe how the initial active power variation of the synchronous machine is reduced to less than one half and the absolute value of its maximum active power variation decreases by approximately 0.4 p.u. when the PV plants employ the SPC. In fact, the beneficial effects are not limited to the period immediately following the disturbance, but the subsequent oscillations are also better damped, with amplitude reductions around 60%.

Both the system frequency and the response of other generating units show that the relative impact of the

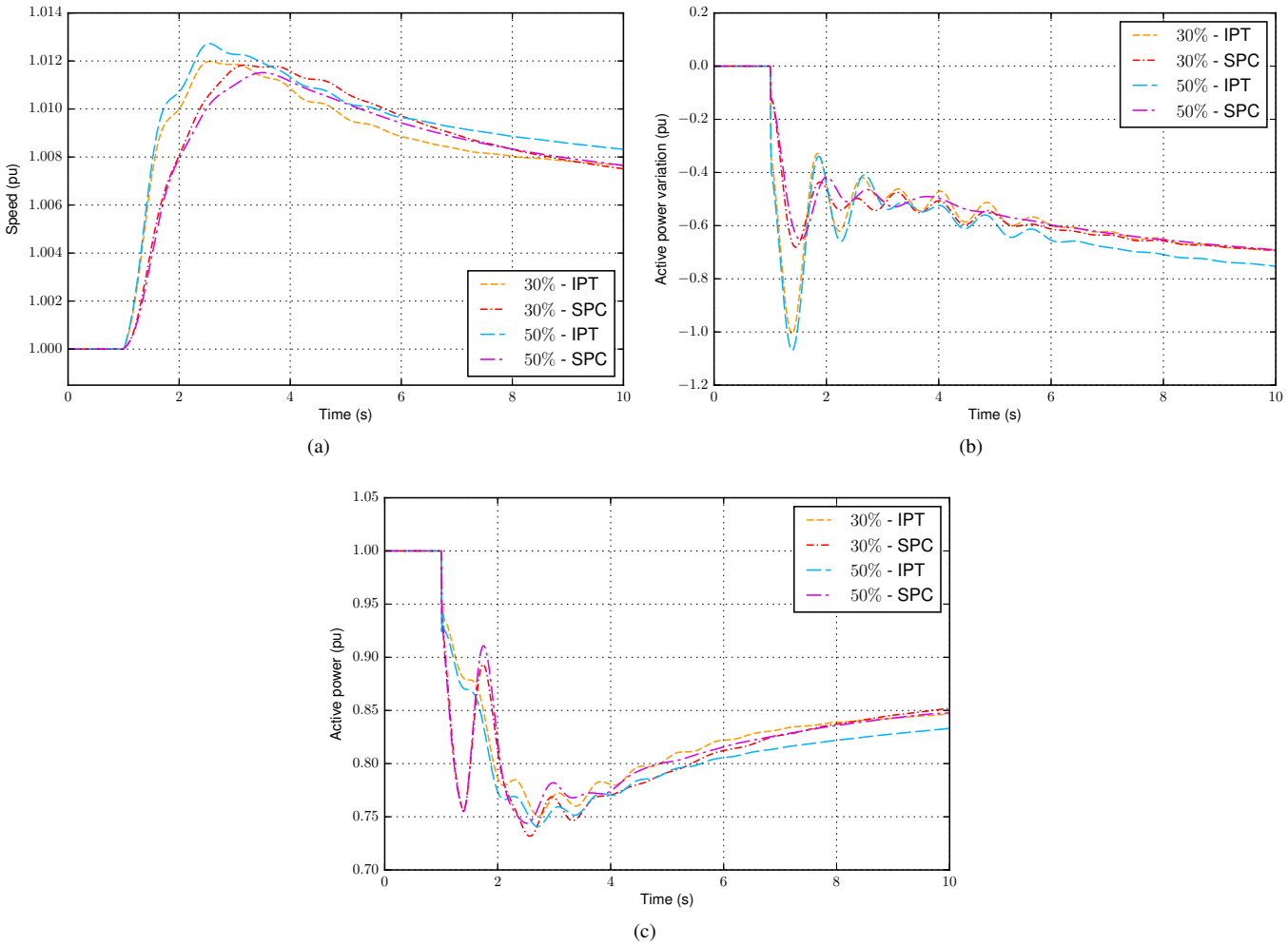

Fig. 6. *12-bus system response to the sudden disconnection of load 4. a) Generator 2 speed. b) Generator 2 active power variation. c) PV plant 1 active power.*

controller is larger in the case of the load disconnection than in the case of the generator disconnection, and this can be explained through Fig. 6c, where the active power response of PV plant 1 is shown. In this case, the plant can reduce its output as set by the SPC and it is not constrained by any active power limitation. Therefore, the disconnection of the load automatically causes a large reduction of the active power injected by the power plant, around 0.25 p.u., when the SPC is used. This response makes a significant difference in the initial frequency slope with respect to the IPT controller, that only modifies the output of the PV plant proportionally to the frequency deviation, which results in a slower response and a faster acceleration of the system. It is worth to mention that the active power reduction determined by both controllers can be achieved due to the fast dynamics of PV systems. Furthermore, this response is naturally stable when the PV plant converters operate in the region of the PV characteristics where the dc voltage is greater or equal than the maximum power point voltage, since any reduction of the output active power results in a dc voltage increase,

which reduces the PV power production, leading to a new equilibrium point.

6. Conclusion

In this paper, the impact on power system stability of PV power plants formed by a number of power converters whose control is based on the SPC has been analysed. With this controller, a converter is able to harmoniously interact with the grid in a similar way to synchronous machines, contributing to its control and stability. The plant inherits these characteristics and has been represented in the analysis by an equivalent single-converter model that includes the SPC and the plant controller.

The study of the small-signal stability of the system shows that there are three critical modes in the system, and their damping ratio increases with the penetration level. This damping ratio improvement is a consequence of the larger number of PV plants connected to the system and able to regulate voltage and frequency. In addition, the eigenvalues that correspond to the least damped mode in the base scenario are visibly affected by the type of converter controller, and the damping of this mode is significantly improved when the SPC is used. Namely, just as a consequence of using the SPC, its damping ratio increases around 2% for a low PV penetration case, and up to 6% when PV plants cover one half of the electricity demand in the system. The time-domain response of the power system shows a reduction in the amplitude and duration of frequency oscillations when the PV penetration increases, and specially for the scenarios considering PV plants with the SPC.

Time-domain simulations of large disturbances affecting the frequency stability of the system are also included in the analysis. On the one hand, the disconnection of a generator proves that PV plants that behave virtually synchronously are able to improve the damping of the system and to reduce the active power oscillations of other generators under such a disturbance, by approximately 30% in the highest penetration scenarios, as long as the plants have a minimum margin to increase their active power output for fractions of a second. On the other hand, the disconnection of a large load allows observing the full contribution of these power plants, without any active power constraints, which results in a decrease of frequency oscillations, and of its maximum deviation up to 10%, as well as a substantial reduction of the effort of the synchronous generators in the system in terms of active power variation and torque oscillations, which can reach values of 60% for a 50% solar penetration level.

Considering these results, PV plants whose power converters are equipped with the SPC can play an interesting role in modern power systems, contributing to voltage and frequency control, but also improving the

damping of oscillations and limiting the maximum deviation of the system frequency when a large disturbance occurs. This contribution, moreover, is shown to be more important as the PV penetration grows. In fact, if certain amount of active power reserve or storage is provided, these power plants are able to contribute to these aspects of the control and stability of the system in a similar way as conventional generating stations.

7. Acknowledgment

This work has been partially supported by the Spanish Ministry of Science and Innovation under the project ENE2014-60228-R.

D. Remon would like to thank the Fundación Bancaria *la Caixa* for supporting his research.

Any opinions, findings and conclusions or recommendations expressed in this material are those of the authors and do not necessarily reflect those of the host institutions or funders.

8. References

[1] International Energy Agency, 'Renewable energy medium-term market report 2016: Executive summary' (IEA Publications, 2016), http://www.iea.org/Textbase/npsum/MTrenew2016SUM.pdf

[2] European Wind Energy Association, 'Wind energy scenarios for 2030' (2015), http://www.ewea.org/fileadmin/files/library/publications/reports/EWEA-Wind-energy-scenarios-2030.pdf

[3] Kabouris, J., Kanellos, F. D.: 'Impacts of large-scale wind penetration on designing and operation of electric power systems', *IEEE Transactions on Sustainable Energy*, 2010, **1**, (2), pp. 107–114

[4] Vittal, E., Keane, A.: 'Identification of critical wind farm locations for improved stability and system planning', *IEEE Transactions on Power Systems*, 2013, **28**, (3), pp. 2950–2958

[5] Eftekharnejad, S., Heydt, G. T., Vittal, V.: 'Optimal generation dispatch with high penetration of photovoltaic generation', *IEEE Transactions on Sustainable Energy*, 2015, **6**, (3), pp. 1013–1020

[6] Martín-Martínez, S., Gómez-Lazaro, E., Molina-Garcia, A., Honrubia-Escribano, A.: 'Impact of wind power curtailments on the Spanish power system operation'. IEEE PES General Meeting, National Harbor, Maryland USA, July 2014, pp. 1–5

[7] Omran, W. A., Kazerani, M., Salama, M. M. A.: 'Investigation of methods for reduction of power fluctuations generated from large grid-connected photovoltaic systems', *IEEE Transactions on Energy Conversion*, 2011, **26**, (1), pp. 318–327

[8] Hossain, M. I., Yan, R., Saha, T. K.: 'Investigation of the interaction between step voltage regulators and large-scale photovoltaic systems regarding voltage regulation and unbalance', *IET Renewable Power Generation*, 2016, **10**, (3), pp. 299–309

[9] Chidurala, A., Saha, T. K., Mithulananthan, N.: 'Harmonic impact of high penetration photovoltaic system on unbalanced distribution networks – learning from an urban photovoltaic network', *IET Renewable Power Generation*, 2016, **10**, (4), pp. 485–494

[10] Kawabe, K., Tanaka, K.: 'Impact of dynamic behavior of photovoltaic power generation systems on short-term voltage stability', *IEEE Transactions on Power Systems*, 2015, **30**, (6), pp. 3416–3424

[11] Edrah, M., Lo, K. L., Anaya-Lara, O.: 'Impacts of high penetration of DFIG wind turbines on rotor angle stability of power systems', *IEEE Transactions on Sustainable Energy*, 2015, **6**, (3), pp. 759–766

[12] Yagami, M., Kimura, N., Tsuchimoto, M., Tamura, J.: 'Power system transient stability analysis in the case of high-penetration photovoltaics'. IEEE PowerTech, Grenoble, France, June 2013, pp. 1–6

[13] Gautam, D., Vittal, V., Harbour, T.: 'Impact of increased penetration of DFIG-based wind turbine generators on transient and small signal stability of power systems', *IEEE Transactions on Power Systems*, 2009, **24**, (3), pp. 1426–1434

[14] Miao, Z.: 'Impact of unbalance on electrical and torsional resonances in power electronic interfaced wind energy systems', *IEEE Transactions on Power Systems*, 2013, **28**, (3), pp. 3105–3113

[15] Eftekharnejad, S., Vittal, V., Heydt, G. T., Keel, B., Loehr, J.: 'Impact of increased penetration of photovoltaic generation on power systems', *IEEE Transactions on Power Systems*, 2013, **28**, (2), pp. 893–901

[16] Nguyen, N., Mitra, J.: 'An analysis of the effects and dependency of wind power penetration on system frequency regulation', *IEEE Transactions on Sustainable Energy*, 2016, **7**, (1), pp. 354–363

[17] Yan, R., Saha, T. K., Modi, N., Masood, N.-A., Mosadeghy, M.: 'The combined effects of high penetration of wind and PV on power system frequency response', *Applied Energy*, 2015, **145**, pp. 320–330

[18] Ghafouri, A., Milimonfared, J., Gharehpetian, G. B.: 'Coordinated control of distributed energy resources and conventional power plants for frequency control of power systems', *IEEE Transactions on Smart Grid*, 2015, **6**, (1), pp. 104–114

[19] Delille, G., Francois, B., Malarange, G.: 'Dynamic frequency control support by energy storage to reduce the impact of wind and solar generation on isolated power system's inertia', *IEEE Transactions on Sustainable Energy*, 2012, **3**, (4), pp. 931–939

[20] Miller, N. W., Clark, K., Shao, M.: 'Frequency responsive wind plant controls: Impacts on grid performance'. IEEE PES General Meeting, Detroit, Michigan USA, July 2011, pp. 1–8

[21] Van Wesenbeeck, M. P. N., De Haan, S. W. H., Varela, P., Visscher, K.: 'Grid tied converter with virtual kinetic storage'. IEEE PowerTech, Bucharest, Romania, June 2009, pp. 1–7

[22] Torres, M., Lopes, L. A. C.: 'Virtual synchronous generator control in autonomous wind-diesel power systems'. IEEE Electrical Power Energy Conference (EPEC), Montreal, Canada, Oct 2009, pp. 1–6

[23] Chen, Y., Hesse, R., Turschner, D., Beck, H.-P.: 'Improving the grid power quality using virtual synchronous machines'. IEEE International Power Engineering, Energy and Electrical Drives (POWERENG), Torremolinos, Spain, May 2011, pp. 1–6

[24] Zhong, Q.-C., Nguyen, P.-L., Ma, Z., Sheng, W.: 'Self-synchronized synchronverters: Inverters without a dedicated synchronization unit', *IEEE Transactions on Power Electronics*, 2014, **29**, (2), pp. 617–630

[25] Shintai, T., Miura, Y., Ise, T.: 'Oscillation damping of a distributed generator using a virtual synchronous generator', *IEEE Transactions on Power Delivery*, 2014, **29**, (2), pp. 668–676

[26] Tamrakar, U., Galipeau, D., Tonkoski, R., Tamrakar, I.: 'Improving transient stability of photovoltaic-hydro microgrids using virtual synchronous machines'. IEEE PowerTech, Eindhoven, Netherlands, June 2015, pp. 1–6

[27] Rodriguez, P., Candela, I., Luna, A.: 'Control of PV generation systems using the synchronous power controller'. IEEE Energy Conversion Congress and Exposition (ECCE), Denver, Colorado USA, Sept 2013, pp. 993–998

[28] Remon, D., Cantarellas, A. M., Elsaharty, M. A. A., Koch-Ciobotaru, C., Rodriguez, P.: 'Synchronous PV support to an isolated power system'. IEEE Energy Conversion Congress and Exposition (ECCE), Montreal, Canada, Sept 2015, pp. 1982–1987

[29] Rodriguez Cortés, P., Candela García, J. I., Rocabert Delgado, J., Teodorescu, R.: 'Synchronous power controller for a generating system based on static power converters', International Patent WO 2012/117131 A1, Sept 2012, Priority date: Feb 18, 2011, Licensed by: Abengoa, S.A.

[30] Remon, D., Cantarellas, A. M., Rodriguez, P.: 'Equivalent model of large-scale synchronous photovoltaic power plants', *IEEE Transactions on Industry Applications*, 2016, **52**, (6), pp. 5029–5040

[31] Jiang, S., Annakkage, U. D., Gole, A. M.: 'A platform for validation of FACTS models', *IEEE Transactions on Power Delivery*, 2006, **21**, (1), pp. 484–491

[32] Adamczyk, A., Altin, M., Goksu, O., Teodorescu, R., Iov, F.: 'Generic 12-bus test system for wind power integration studies'. IEEE European Conference on Power Electronics and Applications (EPE), Lille, France, Sept 2013, pp. 1–6

[33] WECC Renewable Energy Modeling Task Force, 'Generic solar photovoltaic system dynamic simulation model specification' (2012), https://www.wecc.biz/Reliability/WECC%20Solar%20PV%20Dynamic%20Model%20Specification%20-%20September%202012.pdf

[34] Rodriguez, P., Pou, J., Bergas, J., Candela, J., Burgos, R., Boroyevich, D.: 'Decoupled double synchronous reference frame PLL for power converters control', *IEEE Transactions on Power Electronics*, 2007, **22**, (2), pp. 584–592

[35] Kundur, P.: 'Power System Stability and Control' (McGraw-Hill, New York, 1994)